RSC Advances

PAPER

View Article Online
View Journal | View Issue

Cite this: *RSC Adv.*, 2023, **13**, 22503

Synthesis of picolinates *via* a cooperative vinylogous anomeric-based oxidation using UiO-66(Zr)-N($CH_2PO_3H_2$)$_2$ as a catalyst†

Saeed Babaee,[a] Hassan Sepehrmansourie,[a] Mahmoud Zarei,*[b] Mohammad Ali Zolfigol*[a] and Mojtaba Hosseinifard[c]

Received 23rd May 2023
Accepted 18th July 2023

DOI: 10.1039/d3ra03438k

rsc.li/rsc-advances

The anomeric effect highlights the significant influence of the functional group and reaction conditions on oxidation–reduction. This article successfully investigates the anomeric effect in the synthesis of picolinate and picolinic acid derivatives through a multi-component reaction involving 2-oxopropanoic acid or ethyl 2-oxopropanoate, ammonium acetate, malononitrile, and various aldehydes. To facilitate this process, we employed UiO-66(Zr)-N($CH_2PO_3H_2$)$_2$ as a novel nanoporous heterogeneous catalyst. The inclusion of phosphorous acid tags on the UiO-66(Zr)-N($CH_2PO_3H_2$)$_2$ offers the potential for synthesizing picolinates at ambient temperature.

1. Introduction

In recent years, crystal engineering, specifically metal–organic frameworks (MOFs), has gained significant attention across various scientific disciplines. MOFs exhibit diverse applications such as catalysts, photocatalysts, gas separators, oxidizers, adsorbents, and drug delivery systems.[1–5] These frameworks, characterized by high thermal stability and large surface area, have found extensive use as catalysts in coupling, cross-coupling, nitration, multi-component, oxidation-reduction, and Diels–Alder reactions.[6–11] Crystalline porous frameworks consist of an inorganic sector comprising metal cations as nuclei and an organic sector serving as ligand connectors.[12,13] These frameworks possess highly active surfaces and offer a wide range of functional groups, enabling the design of highly efficient catalysts. Notably, their remarkable thermal and chemical stability makes them suitable for various conditions.[14–16] In industries like pharmaceuticals and healthcare, the use of oral and non-toxic materials as catalysts has garnered attention. Among these, phosphoric acid and its derivatives are widely employed in the synthesis of pharmaceutical structures.[17,18] The development of heterogeneous catalysts incorporating phosphoric acid groups has attracted considerable interest due to their recyclability and reusability. Our research group has introduced novel catalysts featuring phosphoric acid tags, including glycoluril,[19] melamine,[20] carbon quantum dots (CQDs),[21] metal–organic frameworks,[22–25] and mesoporous SBA-15.[26] Heterocyclic scaffolds are widely found in a wide range of biological and medicinal active molecules such as anticonvulsant, anticancer, antimicrobial, anti-tumor, antimalarial, antibacterial, antifungal, antitumor and anti-HIV. Pyridine structure such as picolinate and picolinic acid derivatives are used in the pharmaceutical industry due to their biological properties.[27–29] Also, these compounds are used in the formation of complexes with various metals to determine the concentration and in the treatment of diseases as a drug (Fig. 1).[30–36]

Anomeric effect is one of the famous stereoelectronic interactions which has been applied to describe some organic reaction mechanisms.[37–39] The term of anomeric based oxidation (ABO) has been introduced for the formation of final products from susceptible intermediates *via* sharing lone pair electrons of nitrogen atom into the anti-bonding orbitals of C–H bond ($n_N \rightarrow \sigma^*_{C-H}$). This concept has been used as a new strategy for the oxidation of compounds without using any oxidative agent. Stereoelectronic effects have also a major role in the oxidation-reduction of susceptible biological compounds such as NADH/NAD^+ and NADPH/$NADP^+$ (Fig. 2).[40–43]

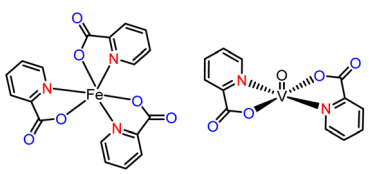

Fig. 1 Structure of picolinic acid complex.

[a]*Department of Organic Chemistry, Faculty of Chemistry, Bu-Ali Sina University, Hamedan 6517838683, Iran. Fax: +988138380709; Tel: +988138282807. E-mail: zolfi@basu.ac.ir; mzolfigol@yahoo.com*

[b]*Department of Chemistry, Faculty of Science, University of Qom, Qom, 37185-359, Iran. E-mail: mahmoud8103@yahoo.com*

[c]*Department of Energy, Materials and Energy Research Center, P.O. Box 31787-316, Karaj, Iran*

† Electronic supplementary information (ESI) available. See DOI: https://doi.org/10.1039/d3ra03438k

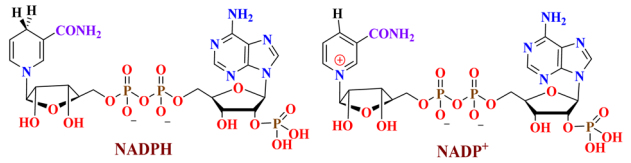

Fig. 2 The molecular structures of NADPH/NADP$^+$.

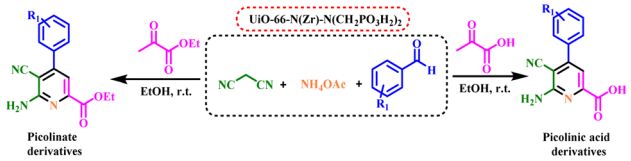

Fig. 3 Synthesis of picolinate and picolinic acid derivatives using UiO-66-N(Zr)-N($CH_2PO_3H_2$)$_2$ as a novel heterogeneous catalyst.

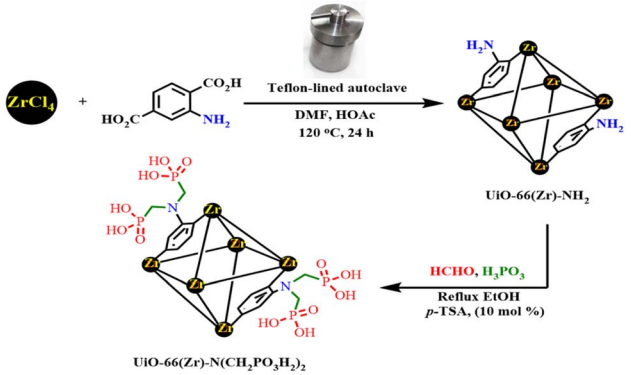

Fig. 4 Synthesis of UiO-66(Zr)-N($CH_2PO_3H_2$)$_2$ as a novel heterogeneous catalyst.

In the continuation of our previous investigation on the applications of catalysts with phosphorous acid tags, herein we decided to design and synthesize UiO-66-N(Zr)-N($CH_2PO_3H_2$)$_2$ as a novel heterogeneous catalyst. Then it was tested for the one-pot synthesis of picolinate and picolinic acid derivatives by condensation reaction of 2-oxopropanoic acid or ethyl 2-oxopropanoate, ammonium acetate, malononitrile and various aldehydes *via* a cooperative anomeric based oxidation mechanism at ambient temperature in ethanol as a solvent (Fig. 3).

2. Experimental

2.1 Materials and methods

All materials and solvents such as 2-amino terephthalic acid (NH_2–H_2BDC), DMF, $ZrCl_4$, methanol, acetone, ethanol, paraformaldehyde, phosphorous acid, *p*-toluene sulfonic acid (*p*-TSA), 2-oxopropanoic acid, ethyl 2-oxopropanoate, acetic acid, ammonium acetate, malononitrile and aldehyde derivatives were purchased from Merck or Sigma-Aldrich and used without further purification.

2.2 General procedure for the preparation of UiO-66(Zr)-N($CH_2PO_3H_2$)$_2$

Firstly, UiO-66(Zr)-NH_2 was synthesized according to the previously reported procedure.[44] Then, by the method of functionalization with phosphorus acid, a mixture of UiO-66(Zr)-NH_2 (0.5 g), formaldehyde (0.06 g, 2 mmol), phosphorus acid (0.164 g, 2 mmol), *p*-TSA (10 mol%, 0.017 g) and ethanol (10 mL) in a 25 mL round-bottomed flask were refluxed for 12 hours. Finally, it was washed with ethanol (2 × 5 mL) and dried under vacuum oven at 80 °C to give UiO-66(Zr)-N($CH_2PO_3H_2$)$_2$ (Fig. 4).

2.3 General procedure for the synthesis of picolinate and picolinic acid derivatives using UiO-66(Zr)-N-($CH_2PO_3H_2$)$_2$

In a 25 mL round-bottomed flask, a mixture of 2-oxopropanoic acid or ethyl 2-oxopropanoate, (1 mmol), aromatic aldehydes (1 mmol), ammonium acetate (1.5 mmol, 0.115 g), malononitrile (1.1 mmol, 0.079 g) and UiO-66(Zr)N($CH_2PO_3H_2$)$_2$ (5 mg) in ethanol (5 mL) as a solvent were stirred at ambient temperature. The progress of the reaction was monitored using TLC (*n*-hexane/ethyl acetate: 2/1). After the completion reaction, the solvent (EtOH) was removed from reaction mixture. Acetone was added to the reaction mixture and the described catalyst was separated using centrifuged (2 × 1000 rpm). Then, solvent was evaporated and the pure product was recrystallized in ethanol (Fig. 3).

2.4 Spectral data for the picolinate and picolinic acid derivatives

Ethyl 6-amino-5-cyano-4-(3-nitrophenyl)picolinate (A1). Yellow solid; Mp: 198–200 °C; IR (KBr): ν (cm^{-1}) = 3473, 3376, 3245, 1732, 1638. ^{1}H NMR (500 MHz, DMSO-d_6) δ (ppm) 8.43 (s, 1H), 8.39 (d, J = 8.0 Hz, 1H), 8.08 (d, J = 7.4 Hz, 1H), 7.86 (t, J = 7.8 Hz, 1H), 7.29 (s, 1H), 7.05 (s, 2H), 4.39 (q, J = 7.2 Hz, 2H), 1.34 (t, J = 7.1 Hz, 3H). ^{13}C NMR (126 MHz, DMSO-d_6) δ (ppm) 163.2, 154.0, 147.8, 147.6, 138.3, 137.0, 135.1, 130.4, 124.3, 123.4, 118.2, 115.0, 114.4, 98.8, 94.8, 62.4, 13.8.

Ethyl 6-amino-5-cyano-4-phenylpicolinate (A2). White solid; Mp: 205–206 °C; IR (KBr): ν (cm^{-1}) = 3426, 3362, 3225, 2925, 2195, 1726, 1670. ^{1}H NMR (500 MHz, DMSO-d_6) δ (ppm) 7.63–7.53 (m, 5H), 7.21 (s, 1H), 6.91 (s, 2H), 4.38 (q, J = 7.3 Hz, 2H), 1.34 (t, J = 7.2 Hz, 3H). ^{13}C NMR (125 MHz, DMSO-d_6) δ (ppm) 163.3, 154.1, 150.0, 136.9, 136.7, 129.7, 128.8, 128.4, 118.2, 115.3, 114.6, 98.6, 62.3, 13.8.

Ethyl 6′-amino-5′-cyano-[3,4′-bipyridine]-2′-carboxylate (A3). Yellow solid; Mp: 242–243 °C; IR (KBr): ν (cm^{-1}) = 3362, 3328, 3154, 2929, 230, 1734, 1671. ^{1}H NMR (500 MHz, DMSO-d_6) δ (ppm) 8.79 (s, 1H), 8.74 (d, J = 3.9 Hz, 1H), 8.06 (d, J = 7.2 Hz, 1H),7.62–7.56 (m, 1H), 7.27 (s, 1H), 7.02 (s, 2H), 4.38 (q, J = 7.2 Hz, 2H), 1.34 (t, J = 7.1 Hz, 3H). ^{13}C NMR (125 MHz, DMSO-d_6) δ (ppm) 163.3, 154.0, 150.5, 148.6, 146.8, 137.1, 136.2, 132.9, 123.6, 118.2, 115.1, 114.4, 98.9, 94.6, 62.3, 13.8.

Ethyl 6-amino-4-(4-chlorophenyl)-5-cyanopicolinate (A4). White solid; Mp: 230–233 °C; IR (KBr): ν (cm^{-1}) = 3465, 3377, 3230, 2924, 2119, 1733, 1635. ^{1}H NMR (500 MHz, DMSO-d_6) δ (ppm) 7.63 (s, 4H), 7.20 (s, 1H), 6.98 (s, 2H), 4.38 (q, J = 7.0 Hz, 2H), 1.34 (t, J = 7.1 Hz, 3H). ^{13}C NMR (125 MHz, DMSO-d_6)

δ (ppm) 163.3, 154.0, 148.7, 136.9, 135.7, 134.7, 130.4, 128.8, 118.1, 115.2, 114.5, 98.6, 62.3, 13.8.

Ethyl 6-amino-5-cyano-4-(3,4-dimethoxyphenyl)picolinate (A5). White solid; Mp: 250–252 °C; IR (KBr): ν (cm^{-1}) = 3389, 3365, 2986, 2217, 1733, 1721. ^{1}H NMR (500 MHz, DMSO-d_6) δ (ppm) 7.23 (s, 1H), 7.22 (s, 1H), 7.17 (d, J = 8.3 Hz, 1H), 7.13 (d, J = 8.1 Hz, 1H), 6.85 (s, 2H), 4.38 (q, J = 6.8 Hz, 2H), 3.84 (s, 3H), 3.83 (s, 3H), 1.35 (t, J = 6.9 Hz, 3H). ^{13}C NMR (125 MHz, DMSO-d_6) δ (ppm) 163.5, 154.1, 149.9, 129.1, 121.3, 118.2, 114.7, 112.2, 111.8, 62.2, 55.7, 55.7, 13.8.

Ethyl 6-amino-5-cyano-4-(4-nitrophenyl) picolinate (A6). Yellow solid; Mp: 205–208 °C; IR (KBr): ν (cm^{-1}) = 3446, 3351, 3248, 3081, 2980, 2213, 1728, 1644, 1530, 1350. ^{1}H NMR (500 MHz, DMSO-d_6) δ (ppm) 8.39 (d, J = 7.6 Hz, 2H), 7.89 (d, J = 7.5 Hz, 2H), 7.25 (s, 1H), 7.06 (s, 2H), 4.38 (d, J = 6.4 Hz, 2H), 1.34 (t, J = 5.9 Hz, 3H). ^{13}C NMR (125 MHz, DMSO-d_6) δ (ppm) 163.2, 154.0, 148.1, 147.8, 143.1, 137.0, 130.1, 130.0, 129.9, 123.8, 123.7, 123.7, 118.0, 114.9, 114.3, 98.6, 95.0, 62.4, 13.8.

Ethyl 6-amino-5-cyano-[4,4′-bipyridine]-2-carboxylate (A7). Yellow solid; Mp: 225–227 °C; IR (KBr): ν (cm^{-1}) = 3336, 3229, 2923, 2220, 1725, 1651. ^{1}H NMR (500 MHz, DMSO-d_6) δ (ppm) 8.39 (d, J = 6.7 Hz, 2H), 7.89 (d, J = 6.6 Hz, 2H), 7.25 (s, 1H), 7.06 (s, 2H), 4.43–4.33 (m, 2H), 1.34 (s, 3H). ^{13}C NMR (125 MHz, DMSO-d_6) δ (ppm) 163.2, 154.0, 148.1, 147.8, 143.1, 137.0, 130.1, 123.8, 118.1, 118.0, 114.9, 114.3, 98.6, 95.0, 62.4, 53.2, 13.8.

Ethyl 6-amino-5-cyano-4-(*p*-tolyl)picolinate (A8). White solid; Mp: 209–210 °C; IR (KBr): ν (cm^{-1}) = 3403, 3318, 3207, 3067, 2224, 1726, 1659. ^{1}H NMR (500 MHz, DMSO-d_6) δ (ppm) 7.50 (d, J = 7.1 Hz, 2H), 7.37 (d, J = 7.1 Hz, 2H), 7.19 (s, 1H), 6.90 (s, 2H), 4.37 (q, J = 6.5, 6.0 Hz, 2H), 2.40 (s, 3H), 1.34 (t, J = 6.6 Hz, 3H). ^{13}C NMR (125 MHz, DMSO-d_6) δ (ppm) 163.4, 154.1, 150.0, 139.5, 136.7, 134.0, 129.4, 128.3, 118.2, 115.4, 114.6, 62.2, 20.8, 13.8.

Ethyl 6-amino-5-cyano-4-(4-cyanophenyl)picolinate (A9). White solid; Mp: 229–231 °C; IR (KBr): ν (cm^{-1}) = 3459, 3330, 3235, 2924, 2229, 2213, 1739, 1634. ^{1}H NMR (500 MHz, DMSO-d_6) δ (ppm) 8.04 (d, J = 7.8 Hz, 2H), 7.81 (d, J = 7.8 Hz, 2H), 7.22 (s, 1H), 7.05 (s, 2H), 4.38 (q, J = 6.6 Hz, 2H), 1.33 (t, J = 6.9 Hz, 3H). ^{13}C NMR (125 MHz, DMSO-d_6) δ (ppm) 163.2, 154.0, 148.2, 141.4, 137.0, 132.7, 129.6, 118.0, 115.0, 114.4, 112.3, 94.8, 62.4, 13.8.

Ethyl 6-amino-5-cyano-4-(thiophen-2-yl)picolinate (A10). Yellow solid; Mp: >300 °C; IR (KBr): ν (cm^{-1}) = 3503, 3444, 3107, 2987, 2230, 1682. ^{1}H NMR (500 MHz, DMSO-d_6) δ (ppm) 7.90 (d, J = 4.0 Hz, 1H), 7.76 (s, 1H), 7.32 (s, 1H), 7.30 (s, 1H), 6.93 (d, J = 13.9 Hz, 2H), 4.39 (d, J = 6.9 Hz, 2H), 1.35 (t, J = 6.8 Hz, 3H). ^{13}C NMR (125 MHz, DMSO-d_6) δ (ppm) 163.1, 154.5, 141.6, 137.5, 136.9, 130.3, 129.6, 128.6, 117.5, 115.6, 114.5, 62.3, 13.8.

6-Amino-4-(4-chlorophenyl)-5-cyanopicolinic acid (B1). Yellow solid; Mp: >300 °C; IR (KBr): ν (cm^{-1}) = 3460, 3363, 3247, 2219, 1716, 1645. ^{1}H NMR (400 MHz, DMSO-d_6) δ (ppm) 7.62 (s, 4H), 7.17 (s, 1H), 6.84 (s, 2H). ^{13}C NMR (101 MHz, DMSO-d_6) δ (ppm) 164.9, 154.0, 148.2, 135.9, 134.5, 130.5, 130.3, 130.2, 128.8, 128.7, 118.2, 115.5, 115.0, 97.4, 94.4.

6-Amino-5-cyano-4-(3,4-dimethoxyphenyl)picolinic acid (B2). Yellow solid; Mp: >300 °C; ^{1}H NMR (400 MHz, DMSO-d_6) δ (ppm) 7.38 (s, 1H), 7.14 (s, 1H), 7.10 (d, J = 1.7 Hz, 2H), 7.07 (s, 1H), 6.26 (s, 2H), 3.83 (s, 3H), 3.82 (s, 3H). ^{13}C NMR (101 MHz, DMSO-d_6) δ (ppm) 165.7, 153.7, 149.5, 148.4, 148.2, 130.2, 121.0, 117.9, 116.7, 116.7, 111.9, 111.6, 94.1, 55.5, 55.5.

6-Amino-5-cyano-4-(4-methoxyphenyl)picolinic acid (B3). Yellow solid; Mp: >300 °C; IR (KBr): ν (cm^{-1}) = 3474, 3359, 3222, 2213, 1720. ^{1}H NMR (400 MHz, DMSO-d_6) δ (ppm) 7.51 (d, J = 8.8 Hz, 2H), 7.41 (s, 1H), 7.08 (d, J = 8.8 Hz, 2H), 7.05 (s, 1H), 6.28 (s, 2H), 3.83 (s, 3H). ^{13}C NMR (101 MHz, DMSO-d_6) δ (ppm) 165.8, 159.9, 153.7, 149.8, 148.0, 130.1, 129.7, 118.0, 116.6, 116.6, 114.1, 94.1, 93.8, 55.2.

6-Amino-5-cyano-4-phenylpicolinic acid (B4). Yellow solid; Mp: >300 °C; IR (KBr): ν (cm^{-1}) = 3446, 3365, 2926, 2211, 1630, 1575. ^{1}H NMR (400 MHz, DMSO-d_6) δ (ppm) 7.52 (d, J = 7.5 Hz, 5H), 7.35 (s, 2H), 7.12 (s, 1H), 6.39 (s, 2H). ^{13}C NMR (101 MHz, DMSO-d_6) δ (ppm) 166.3, 153.7, 148.4, 137.9, 129.1, 128.6, 128.3, 127.6, 118.3, 116.4, 116.3, 94.7, 94.4.

6-Amino-5-cyano-[4,4′-bipyridine]-2-carboxylic acid (B5). Yellow solid; Mp: >300 °C; IR (KBr): ν (cm^{-1}) = 3360, 2217, 1647, 1389. ^{1}H NMR (400 MHz, DMSO-d_6) δ (ppm) 8.75–8.70 (m, 2H), 7.60–7.54 (m, 2H), 7.39 (s, 1H), 7.08 (s, 1H), 6.47 (s, 2H). ^{13}C NMR (101 MHz, DMSO-d_6) δ (ppm) 165.3, 153.6, 150.5, 150.0, 145.5, 145.4, 123.0, 117.7, 116.3, 115.9, 95.8, 93.5.

6-Amino-5-cyano-4-(4-hydroxyphenyl)picolinic acid (B6). Yellow solid; Mp: >300 °C; IR (KBr): ν (cm^{-1}) = 3609, 34.8, 3347, 3213, 2213, 1639. ^{1}H NMR (400 MHz, DMSO-d_6) δ (ppm) 7.69–7.33 (m, 5H), 7.13 (s, 2H), 6.81 (s, 2H). ^{13}C NMR (101 MHz, DMSO) δ (ppm) 167.3, 167.2, 161.8, 158.4, 116.4, 115.3, 79.1, 70.4.

3. Results and discussion

Based on our previous experiences and our knowledge related of the catalytic applications on the development of the cooperative vinylogous anomeric-based oxidation concept,[37–39] we wish to report a novel heterogeneous catalyst [UiO-66(Zr)-N($CH_2PO_3H_2$)$_2$] containing phosphorous acid groups as a non-toxic, high efficiency and stable catalyst. The above said

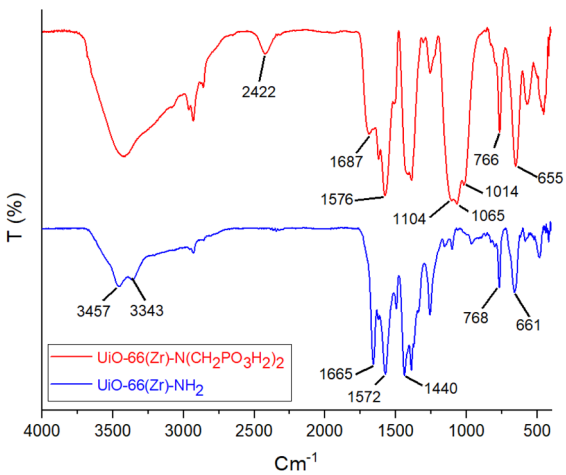

Fig. 5 The comparison of FT-IR of UiO-66(Zr)-NH_2 and UiO-66(Zr)-N($CH_2PO_3H_2$)$_2$ as a novel heterogeneous catalyst.

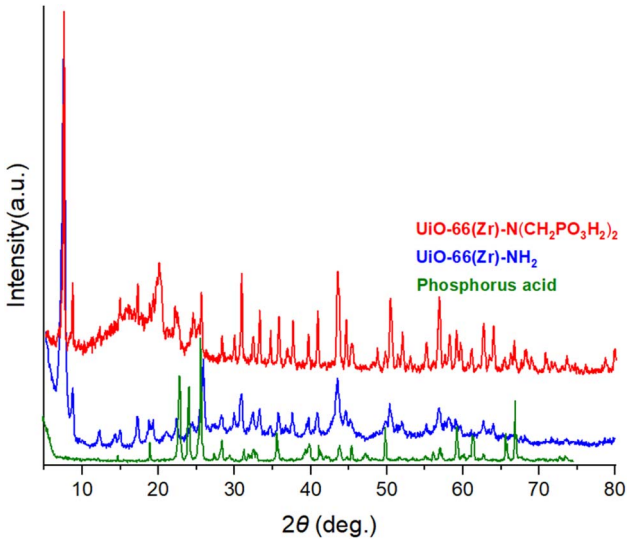

Fig. 6 XRD pattern of phosphorus acid, UiO-66(Zr)-NH_2 and UiO-66(Zr)-$N(CH_2PO_3H_2)_2$ as a novel heterogeneous catalyst.

catalyst was fully characterized by methods such as Fourier transform infrared spectroscopy (FT-IR), elemental mapping analysis (EDX), the scanning electron microscope (SEM) and X-ray spectroscopy (XRD). Also, UiO-66(Zr)-$N(CH_2PO_3H_2)_2$ was applied for the synthesis of new picolinate and picolinic acid derivatives under mild reaction.

The FT-IR spectra of UiO-66(Zr)-NH_2 and UiO-66(Zr)-$N(CH_2PO_3H_2)_2$ were compared in Fig. 5. The broad peak 2800–3500 cm^{-1} is related to OH of PO_3H_2 groups. Then, the absorption bands at 1014 and 1065 cm^{-1} are related to P–O bond stretching and the band at 1104 cm^{-1} is related to P=O.[45] Furthermore, peaks of Zr–O–Zr and Zr–O appeared at 766 and 655 cm^{-1}, respectively. The FT-IR spectrum difference between UiO-66(Zr)-NH_2 and UiO-66(Zr)-$N(CH_2PO_3H_2)_2$ verified the structure of the catalyst.

The XRD analysis of phosphorus acid, UiO-66(Zr)-NH_2 and UiO-66(Zr)-$N(CH_2PO_3H_2)_2$ were shown in the range of $2\theta = 5$–80 (Fig. 6). The comparison results of the XRD spectrum of UiO-66(Zr)-$N(CH_2PO_3H_2)_2$ and UiO-66(Zr)-NH_2 show that it has the same pattern and morphology. Also, by comparing the XRD spectrum of UiO-66(Zr)-$N(CH_2PO_3H_2)_2$ and phosphorus acid, the presence of phosphorus acid peaks is observed in the

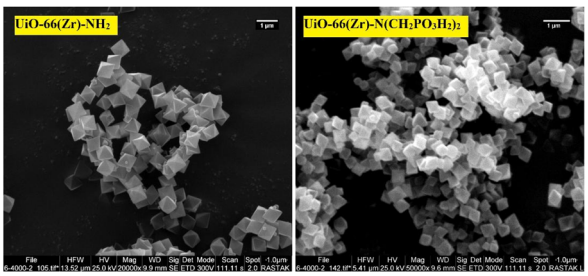

Fig. 7 SEM images of UiO-66(Zr)-NH_2 and UiO-66(Zr)-$N(CH_2PO_3H_2)_2$.

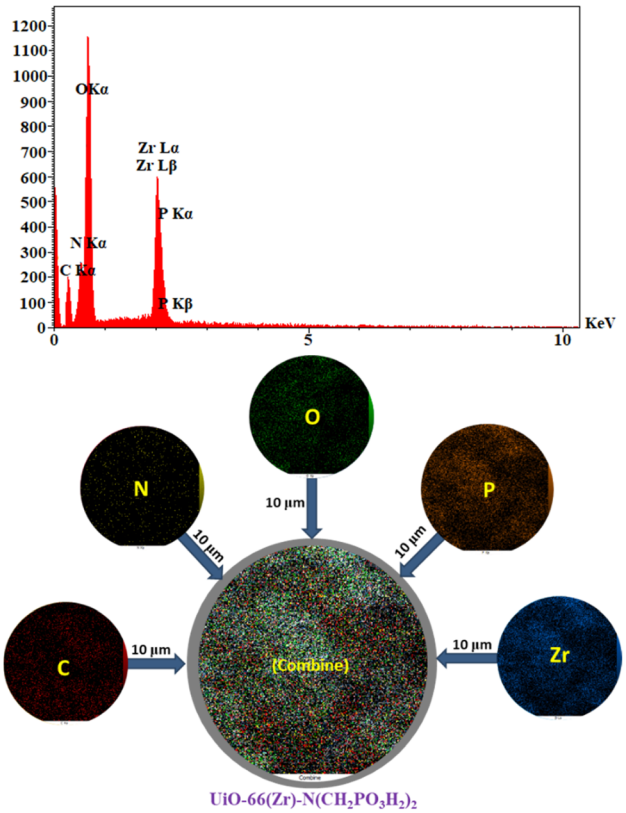

Fig. 8 Energy-dispersive X-ray spectroscopy (EDX) and elemental mapping of C (red), Zr (blue), N (yellow), O (green) and P (orange) atoms for UiO-66(Zr)-$N(CH_2PO_3H_2)_2$ as a novel heterogeneous catalyst.

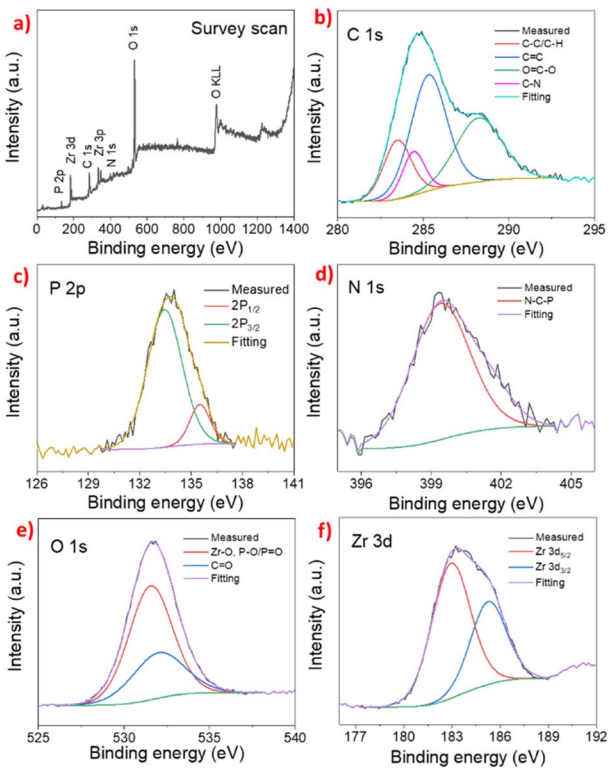

Fig. 9 XPS spectra of the UiO-66(Zr)-$N(CH_2PO_3H_2)_2$: (a) full scan, (b) C 1s, (c) P 2p, (d) N 1s, (e) O 1s and (f) Zr 3d.

Table 1 Effect of different amounts of catalysts, temperature and solvent (5 mL) in the synthesis of picolinate and picolinic acid derivatives

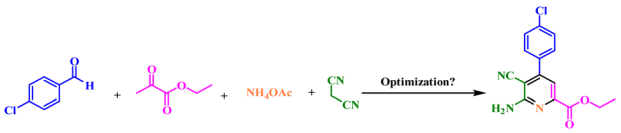

Entry	Catalyst (mg)	Solvent	Temperature (°C)	Time (min)	Yield (%)
1	5	DMF	100	60	80
2	5	H_2O	Reflux	120	25
3	5	*n*-Hexane	Reflux	120	—
4	5	CH_3CN	Reflux	120	60
5	5	$CHCl_3$	Reflux	180	50
6	5	CH_2Cl_2	Reflux	150	—
7	5	EtOAc	Reflux	180	—
8	5	MeOH	Reflux	180	45
9	5	EtOH	Reflux	100	60
10	5	EtOH	50	80	72
11	5	EtOH	25	60	88
12	2.5	EtOH	25	80	70
13	10	EtOH	25	60	88
14	—	EtOH	25	60	Trace
15	5	—	25	180	—
16	5	—	100	100	25

structure of UiO-66(Zr)-N$(CH_2PO_3H_2)_2$. The XRD of UiO-66(Zr)-N$(CH_2PO_3H_2)_2$ showed that it still retained a crystalline structure after the functionalized process. In another study, the morphology of UiO-66(Zr)-NH_2 and UiO-66(Zr)-N$(CH_2PO_3H_2)_2$ can be seen by scanning electron microscope (SEM) (Fig. 7). Comparing the SEM images of UiO-66(Zr)-N$(CH_2PO_3H_2)_2$ and UiO-66(Zr)-NH_2 shows that the morphology has not changed after functionalization. According to SEM images, the particles of UiO-66(Zr)-N$(CH_2PO_3H_2)_2$ were uniform size with good dispersion performance and no agglomeration.

In energy-dispersive X-ray spectroscopy (EDX) and elemental mapping analysis zirconium, nitrogen, oxygen, carbon and phosphor atoms were confirmed in the structure of UiO-66(Zr)-N$(CH_2PO_3H_2)_2$ (Fig. 8). Furthermore, the well-dispersed distribution of elements in the UiO-66(Zr)-N$(CH_2PO_3H_2)_2$ was determined and verified by elemental mapping (Fig. 8).

The elements and their chemical environments of the prepared samples were characterized by X-ray photoelectron spectroscopy (XPS) and the results are depicted in Fig. 9. The survey scan of UiO-66(Zr)-N$(CH_2PO_3H_2)_2$ revealed the co-existence of phosphor, carbon, nitrogen, oxygen, and zirconium (Fig. 9a), which confirms loading of phosphorous functional group on the surface of UiO-66(Zr)-NH_2. High-resolution XPS of C 1s demonstrated four peaks located at 283.6, 284.6, 285.4, and 288.5 eV, which respectively correspond to the C–C/C–H, C–N, C=C and C=O species (Fig. 9b). Moreover, P 2p peaks cantered at binding energies of 133.4 and 135.5 eV revealing P $2p_{3/2}$ and P $2p_{1/2}$, respectively (Fig. 9c), the shift of binding energies for P to higher energies reveals bonding of phosphorus to oxygen and clearly shows the presence of bonded phosphorus acid. High-resolution XPS of N 1s demonstrated one peak located at 399.6 eV which correspond to the N–C–P specie (Fig. 9d). Moreover, O 1s contains peaks binding energies at 531.6 and 532.3 eV revealing Zr–O and C=O, respectively (Fig. 9e). Since the peak cantered at 531.6 eV is very intense and broad it belongs to Zr–O, P–O and P=O. As shown in Fig. 9f, the Zr 3d XPS spectrum contains two peaks at 182.9 and 185.3 eV, belonging to Zr $3d_{5/2}$ and Zr $3d_{3/2}$, respectively.[46–48]

After the structure and morphology of UiO-66(Zr) N$(CH_2PO_3H_2)_2$ were determined, it was used as a heterogeneous catalyst for the synthesis of picolinate and picolinic acid

Table 2 Evaluation of various catalyst for the synthesis of picolinate and picolinic acid derivatives in comparison with UiO-66(Zr)-N$(CH_2PO_3H_2)_2$ in ethanol under room temperature conditions

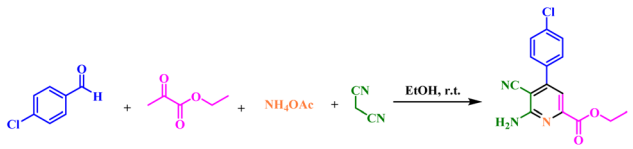

Entry	Catalyst	Amount of catalyst	Time (min)	Yield (%)
1	[Py-SO_3H]Cl (ref. 49)	10 mol%	120	40
2	Fe_3O_4	10 mg	120	—
3	$Al(HSO_4)_3$	10 mol%	90	45
4	$H_3[P(W_3O_{10})_4]\cdot XH_2O$	10 mol%	80	50
5	*p*-TSA	10 mol%	60	60
6	SSA (ref. 50 and 51)	10 mg	80	35
7	GTBSA (ref. 52)	10 mol%	70	58
8	[PVI-SO_3H]Cl (ref. 53)	10 mol%	65	70
9	UiO-66-NH_2	5 mg	120	24
10	H_3PO_4	10 mol%	80	70
11	UiO-66-N$(CH_2PO_3H_2)_2$	5 mg	60	88
12	H_3PO_3	5 mol%	85	70

derivatives. In order to synthesize picolinate and picolinic acid derivatives, the reaction of between ethyl 2-oxopropanoate (1 mmol, 0.116 g), ammonium acetate (1.5 mmol, 0.115 g), malononitrile (1.2 mmol, 0.079 g) and 4-chlorobenzaldehyde (1 mmol, 0.140 g) was selected as a model reaction for optimization of amount of catalyst, solvent and temperature. The reaction was investigated in several solvents (5 mL) such as DMF, H_2O, *n*-hexane, CH_3CN, EtOH, $CHCl_3$, CH_2Cl_2, EtOAc, MeOH (Table 1, entries 1–10) and without solvent (Table 1, entries 15–16) in the presence of 5 mg UiO-66(Zr)-$N(CH_2PO_3H_2)_2$. The model reaction was also studied in different amount of catalyst and temperature (Table 1, entries 9–14). The best choice for the synthesis of picolinate and picolinic acid derivatives was achieved in the presence of 5 mg UiO-66(Zr)-$N(CH_2PO_3H_2)_2$ in EtOH as solvent at ambient temperature (Table 1, entry 11).

To evaluate the performance of UiO-66(Zr)-$N(CH_2PO_3H_2)_2$ as a catalyst for the preparation picolinate and picolinic acid derivatives, we have used various homogeneous and heterogeneous catalysts for the condensation reaction ethyl 2-oxopropanoate (1 mmol, 0.116 g), ammonium acetate (1.5 mmol, 0.115 g), malononitrile (1.2 mmol, 0.079 g), in Table 2. As shown Table 2, UiO-66(Zr)-$N(CH_2PO_3H_2)_2$ is the best catalyst for the synthesis of picolinate and picolinic acid derivatives.

After optimization of the reaction conditions and evaluation of the performance of catalyst for the synthesis picolinic derivatives, a wide range of aromatic aldehydes including electron withdrawing, electron releasing and heterocyclic rings

Table 3 Synthesis of picolinate and picolinic acid derivatives using UiO-66(Zr)-$N(CH_2PO_3H_2)_2$ as porous catalyst

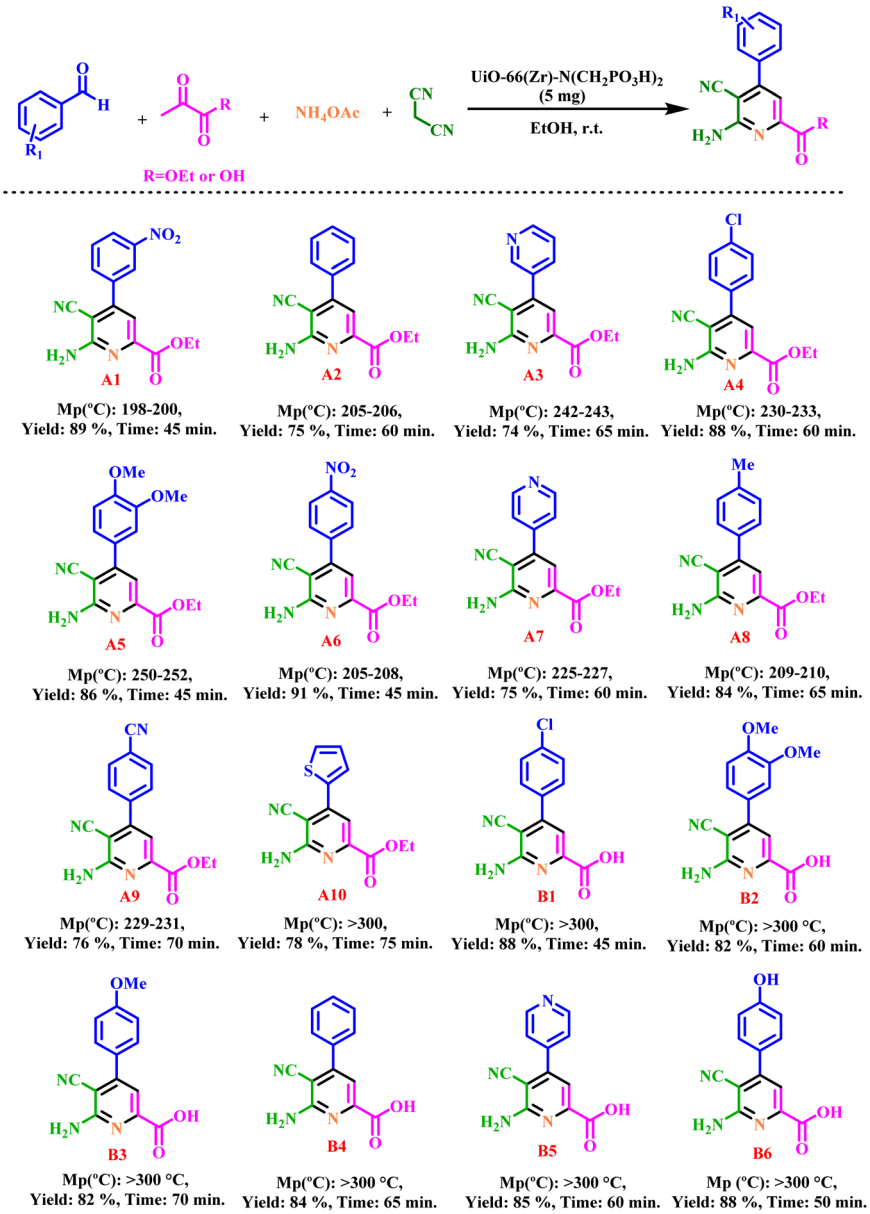

were tested to obtain desired products (Table 3). As shown in Table 3, the obtained results indicated that UiO-66(Zr)-$N(CH_2PO_3H_2)_2$ is appropriate for the preparation of target molecules in high to excellent yields (74–91%) with relatively short reaction times (45–75 min).

Proposed mechanism for the synthesis of picolinate and picolinic acid derivatives using UiO-66(Zr)-$N(CH_2PO_3H_2)_2$ has been summarized in Fig. 10. First, aldehyde is activated by (–OH) of PO_3H_2 group. Then, this substrate is reacted with malononitrile to lose one molecule of water, to give intermediate (**I**). Simultaneously, ethyl pyruvate reacts with the NH_3 released from ammonium acetate to give intermediate (**II**). In the next step, intermediate (**II**) reacts with intermediate (**I**), as a Michael acceptor, to give intermediate **(III)**. Intermediate (**III**) is converted to intermediate (**VI**) through tautomerization and intramolecular cyclization. Then, the hydride or hydrogen peroxide, respectively released from intermediate (**VI**) *via* interaction of lone pair electrons of N atoms and C=C bonds. Finally, the 1,4-dihydropyridines converts to their

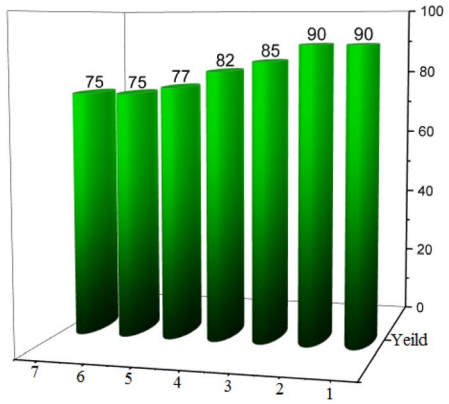

Fig. 11 Recyclability of UiO-66(Zr)-$N(CH_2PO_3H_2)_2$ as novel heterogeneous catalyst for the synthesis of picolinate and picolinic acid derivatives.

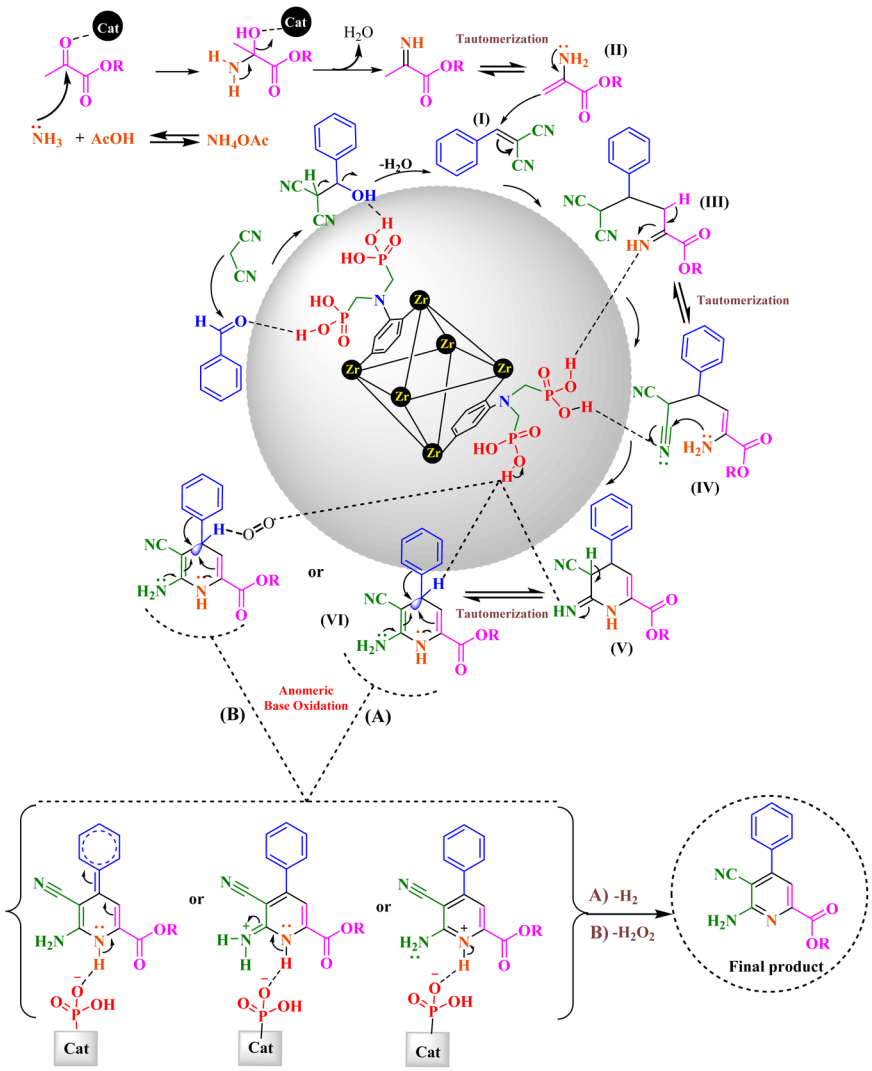

Fig. 10 Proposed mechanism for the synthesis of picolinate and picolinic acid derivatives using UiO-66(Zr)-$N(CH_2PO_3H_2)_2$ as a novel heterogeneous catalyst.

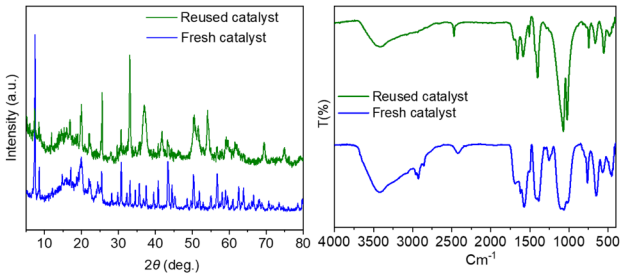

Fig. 12 Comparison of FT-IR and XRD spectra of fresh and recovered catalyst.

corresponding picolinate and picolinic acid derivatives *via* a cooperative vinylogous anomeric based oxidation and releases a hydrogen ($-H_2$) or hydrogen peroxide ($-H_2O_2$) molecules.[22,54] The obtained results of the model reaction under argon, nitrogen and oxygen atmospheres are similar which are verified presented mechanism (Fig. 10).

The recyclability and reusing of UiO-66(Zr)-$N(CH_2PO_3H_2)_2$ was studied in the synthesis of picolinate and picolinic acid derivatives by reaction of ethyl 2-oxopropanoate (1 mmol, 0.116 g), ammonium acetate (1.5 mmol, 0.115 g), malononitrile (1.2 mmol, 0.079 g) and 4-chlorobenzaldehyde (1 mmol, 0.140 g) as a model reaction under the above-mentioned optimized reaction conditions. As indicated in Fig. 11, UiO-66(Zr)-$N(CH_2PO_3H_2)_2$ can be reused up to six times without noticeable changes in its catalytic activity.

The structure and morphology of the recovered catalyst after seven times of use were investigated using FT-IR and XRD techniques. The results of FT-IR and XRD analyses show that the structure and morphology have not changed after using (Fig. 12).

4. Conclusions

In summary, we have synthesized a new porous heterogeneous catalyst, which is a new metal organic framework containing phosphorous acid tags. Identification techniques was used for the approving the desired catalyst structure. UiO-66(Zr)-$N(CH_2PO_3H_2)_2$ was used as a heterogeneous catalyst for the one-pot synthesis of new picolinate and picolinic acid derivatives under ambient temperature in EtOH. Examining the reaction mechanism shows that in the final stage, the intermediate was transformed into the final product *via* a cooperative vinylogous anomeric based oxidation mechanism.

Conflicts of interest

The authors declare no competing financial interests.

Acknowledgements

We thank the Bu-Ali Sina University and Iran National Science Foundation (INSF) (Grant Number: 98001912) for financial support.

References

1 C. Vaitsis, G. Sourkouni and C. Argirusis, *Ultrason. Sonochem.*, 2019, **52**, 106–119.
2 (*a*) P. P. Bag, G. P. Singh, S. Singha and G. Roymahapatra, *Eng. Sci.*, 2020, **13**, 1–10; (*b*) K. Suresh and A. J. Matzger, *Angew Chem. Int. Ed. Engl.*, 2019, **58**, 16790–16794.
3 H. Li, K. Wang, Y. Sun, C. T. Lollar, J. Li and H. C. Zhou, *Mater. Today*, 2018, **21**, 108–121.
4 (*a*) N. Stock and S. Biswas, *Chem. Rev.*, 2012, **112**, 933–969; (*b*) H. Sepehrmansourie, H. Alamgholiloo, N. N. Pesyan and M. A. Zolfigol, *Appl. Catal., B*, 2023, **321**, 122082.
5 (*a*) S. Kitagawa, *Chem. Soc. Rev.*, 2014, **43**, 5415–5418; (*b*) H. Sepehrmansourie, H. Alamgholiloo, M. A. Zolfigol, N. N. Pesyan and M. M. Rasooll, *ACS Sustainable Chem. Eng.*, 2023, **11**, 3182–3193.
6 S. Wang, C. M. McGuirk, A. d'Aquino, J. A. Mason and C. A. Mirkin, *Adv. Mater.*, 2018, **30**, 1800202.
7 L. Jiao, Y. Wang, H. L. Jiang and Q. Xu, *Adv. Mater.*, 2018, **30**, 1703663.
8 (*a*) Q. Yang and H. L. Jiang, *Small Methods*, 2018, **2**, 1800216; (*b*) H. Sepehrmansourie, M. Zarei, M. A. Zolfigol, S. Kalhor and H. Shi, *Mol. Catal.*, 2022, **531**, 112634; (*c*) B. Danishyar, H. Sepehrmansourie, H. Ahmadi, M. Zarei, M. A. Zolfigol and M. Hosseinifard, *ACS Omega*, 2023, **8**, 18479–18490.
9 B. Gole, A. K. Bar, A. Mallick, R. Banerjee and P. S. Mukherjee, *Chem. Commun.*, 2013, **49**, 7439–7441.
10 F. Ghamari, D. Raoufi, S. Alizadeh, J. Arjomandi and D. Nematollahi, *J. Mater. Chem. A*, 2021, **9**, 15381–15393.
11 J. Dou, C. Zhu, H. Wang, Y. Han, S. Ma, X. Niu and Q. Chen, *Adv. Mater.*, 2021, **33**, 2102947.
12 J. Kujawa, S. Al-Gharabli, T. M. Muzioł, K. Knozowska, G. Li, L. F. Dumée and W. Kujawski, *Coord. Chem. Rev.*, 2021, **440**, 213969.
13 J. Feng, W. X. Ren, F. Kong and Y. B. Inorg, *Chem. Front.*, 2021, **8**, 848–879.
14 (*a*) H. Sepehrmansourie, *Iran. J. Catal.*, 2021, **11**, 207–215; (*b*) F. Jalili, M. Zarei, M. A. Zolfigol and A. Khazaei, *RSC Adv.*, 2022, **12**, 9058–9068.
15 (*a*) H. Sepehrmansourie, M. Zarei, M. A. Zolfigol, S. Babaee and S. Rostamnia, *Sci. Rep.*, 2021, **11**, 5279; (*b*) Z. Torkashvand, H. Sepehrmansourie, M. A. Zolfigol and M. A. As' Habi, *Mol. Catal.*, 2023, **541**, 113107.
16 S. Zhang, X. Zhao, H. Niu, Y. Shi, Y. Cai and G. Jiang, *J. Hazard. Mater.*, 2009, **167**, 560–566.
17 Y. D. Shao and D. J. Cheng, *ChemCatChem*, 2021, **13**, 1271–1289.
18 M. Terada, *Chem. Commun.*, 2008, **35**, 4097–4112.
19 (*a*) S. Moradi, M. A. Zolfigol, M. Zarei, D. A. Alonso and A. Khoshnood, *ChemistrySelect*, 2018, **3**, 3042–3047; (*b*) B. Danishyar, H. Sepehrmansourie, M. Zarei, M. A. Zolfigol, M. A. As' Habi and Y. Gu, *Polycyclic Aromat. Compd.*, 2022, 1–21.
20 J. Afsar, M. A. Zolfigol, A. Khazaei, M. Zarei, Y. Gu, D. A. Alonso and A. Khoshnood, *Mol. Catal.*, 2020, **482**, 110666.

21 M. M. Rasooll, M. Zarei, M. A. Zolfigol, H. Sepehrmansourie, A. Omidi, M. Hasani and Y. Gu, *RSC Adv.*, 2021, **11**, 25995–26007.
22 (*a*) S. Kalhor, M. Zarei, H. Sepehrmansourie, M. A. Zolfigol, H. Shi, J. Wang, J. Arjomandi, M. Hasani and R. Schirhagl, *Mol. Catal.*, 2021, **507**, 111549; (*b*) E. Tavakoli, H. Sepehrmansourie, M. Zarei, M. A. Zolfigol, A. Khazaei and M. Hosseinifard, *New J. Chem.*, 2022, **46**, 19054–19061.
23 (*a*) H. Sepehrmansouri, M. Zarei, M. A. Zolfigol, A. R. Moosavi-Zare, S. Rostamnia and S. Moradi, *Mol. Catal.*, 2020, **481**, 110303; (*b*) H. Sepehrmansourie, M. Zarei, M. A. Zolfigol, S. Babaee, S. Azizian and S. Rostamnia, *Sci. Rep.*, 2022, **12**, 14145.
24 (*a*) S. Kalhor, M. Zarei, M. A. Zolfigol, H. Sepehrmansourie, D. Nematollahi, S. Alizadeh and J. Arjomandi, *Sci. Rep.*, 2021, **11**, 19370; (*b*) M. Mohammadi Rasooll, H. Sepehrmansourie, M. Zarei, M. A. Zolfigol, M. Hosseinifard and Y. Gu, *ACS Omega*, 2023, **8**, 25303–25315.
25 S. Babaee, M. Zarei, H. Sepehrmansourie, M. A. Zolfigol and S. Rostamnia, *ACS Omega*, 2020, **5**, 6240–6249.
26 F. Jalili, M. Zarei, M. A. Zolfigol, S. Rostamnia and A. R. Moosavi-Zare, *Microporous Mesoporous Mater.*, 2020, **294**, 109865.
27 P. Koczoń, J. Piekut, M. Borawska, R. Świsłocka and W. Lewandowski, *Anal. Bioanal. Chem.*, 2006, **384**, 302–308.
28 P. Koczoń, J. Piekut, M. Borawska, R. Świsłocka and W. Lewandowski, *Spectrochim. Acta, Part A*, 2005, **61**, 1917–1922.
29 C. F. Ramogida, A. K. Robertson, U. Jermilova, C. Zhang, H. Yang, P. Kunz, J. Lassen, I. Bratanovic, V. Brown, L. Southcott and C. Rodríguez-Rodríguez, *EJNMMI radiopharm. chem.*, 2019, **4**, 1–20.
30 R. March, W. Clegg, R. A. Coxall, L. Cucurull-Sánchez, L. Lezama, T. Rojo and P. González-Duarte, *Inorg. Chim. Acta*, 2003, **353**, 129–138.
31 R. J. Beninger, A. M. Colton, J. L. Ingles, K. Jhamandas and R. J. Boegman, *Neuroscience*, 1994, **61**, 603–612.
32 H. L. Seng, S. T. Von, K. W. Tan, M. J. Maah, S. W. Ng, R. N. Z. R. A. Rahman, I. Caracelli and C. H. Ng, *Biometals*, 2010, **23**, 99–118.
33 R. R. Pulimamidi, R. Nomula, R. Pallepogu and H. Shaik, *Eur. J. Med. Chem.*, 2014, **79**, 117–127.
34 J. A. Davis and J. O. Leckie, *Environ. Sci. Technol.*, 1978, **12**, 1309–1315.
35 K. Grossmann, F. Scheltrup, J. Kwiatkowski and G. Caspar, Induction of abscisic acid is a common effect of auxin herbicides in susceptible plants, *J. Plant Physiol.*, 1996, **149**, 475–478.
36 J. W. Hamaker, H. Johnston, R. T. Martin and C. T. Redemann, A picolinic acid derivative: plant Growth Regul, *Science*, 1963, **141**, 363.
37 F. Zhu and M. A. Walczak, *J. Am. Chem. Soc.*, 2020, **142**, 15127–15136.
38 C. A. Tsipis, E. G. Bakalbassis, S. A. Zisopoulou and J. K. Gallos, *Org. Biomol. Chem.*, 2021, **19**, 1066–1082.
39 (*a*) I. V. Alabugin, L. Kuhn, M. G. Medvedev, N. V. Krivoshchapov, V. A. Vil, I. A. Yaremenko, P. Mehaffy, M. Yarie, A. O. Terent'ev and M. A. Zolfigol, *Chem. Soc. Rev.*, 2021, **50**, 10253–10345; (*b*) H. Sepehrmansourie, M. Mohammadi Rasooll, M. Zarei, M. A. Zolfigol and Y. Gu, *Inorg. Chem.*, 2023, **62**, 9217–9229; (*c*) E. Tavakoli, H. Sepehrmansourie, M. Zarei, M. A. Zolfigol, A. Khazaei and M. A. As' Habi, *Sci. Rep.*, 2023, **13**, 9388.
40 X. Zhao, J. Xiao and W. Tang, *Synthesis*, 2017, **49**, 3157–3164.
41 C. B. Bai, N. X. Wang, Y. Xing and X. W. Lan, Progress on chiral NAD(P)H model compounds, *Synlett*, 2017, **28**, 402–414.
42 T. He, R. Shi, Y. Gong, G. Jiang, M. Liu, S. Qian and Z. Wang, *Synlett*, 2016, **27**, 1864–1869.
43 G. Hamasaka, H. Tsuji and Y. Uozumi, *Synlett*, 2015, **26**, 2037–2041.
44 M. Chen, Y. Tu and S. Wu, *Mater*, 2021, **14**, 2419.
45 V. Jagodić, *Croat. Chem. Acta*, 1977, **49**, 127–133.
46 M. Peñas-Garzón, M. J. Sampaio, Y. L. Wang, J. Bedia, J. J. Rodriguez, C. Belver, C. G. Silva and J. L. Faria, *Sep. Purif.*, 2022, **286**, 120467.
47 B. Peng, Y. Xu, K. Liu, X. Wang and F. M. Mulder, *ChemElectroChem*, 2017, **4**, 2140–2144.
48 X. Sui, X. Huang, H. Pu, Y. Wang and J. Chen, *Nano Energy*, 2021, **83**, 105797.
49 A. R. Moosavi-Zare, M. A. Zolfigol, M. Zarei, A. Zare, V. Khakyzadeh and A. Hasaninejad, *Appl. Catal., A*, 2013, **467**, 61–68.
50 M. A. Zolfigol, *Tetrahedron*, 2001, **57**, 9509–9511.
51 H. Sepehrmansourie, *Iran. J. Catal.*, 2020, **10**, 175–179.
52 M. Zarei, H. Sepehrmansourie, M. A. Zolfigol, R. Karamian and S. H. Moazzami Farida, *New J. Chem.*, 2018, **42**, 14308–14317.
53 H. Sepehrmansourie, M. Zarei, R. Taghavi and M. A. Zolfigol, *ACS Omega*, 2019, **4**, 17379–17392.
54 (*a*) A. M. Naseri, M. Zarei, S. Alizadeh, S. Babaee, M. A. Zolfigol, D. Nematollahi, J. Arjomandi and H. Shi, *Sci. Rep.*, 2021, **11**, 16817; (*b*) H. Sepehrmansourie, S. Kalhor, M. Zarei, M. A. Zolfigol and M. Hosseinifard, *RSC Adv.*, 2022, **12**, 34282–34292.